Topological Analysis on the Dispersion Polymerization of Styrene in Ethanol

Jung Mo Son and Hyungsuk Pak*

Department of Chemistry, Seoul National University, Seoul 151-742, Korea
Received November 6, 1995

A topological theory has been introduced to explain and evaluate the fractional volumes of system materials, the change of the weight and concentration of monomer molecules, molecular weight distribution, and interaction functions of polymer-polymer and polymer-oligomer, etc. for dispersion polymerization. The previous theory of Lu *et al.* has offered only an incomplete simulation model for dispersion polymer systems, whereas our present one gives a general theoretical model applicable to all the polymerization systems. The theory of Lu *et al.* considered only the physical property term caused by interaction between matters of low molecular weight (*i.e.*, diluent, monomer, and oligomer) and polymer particles without dealing with physical properties caused by the structure of polymer networks in polymer particles, while our theory deals with all physical effect possible, caused by the displacement of not only entangled points but also junction points in polymer particles. The theoretically predictive values show good agreement with the experimental data for dispersion polymerization systems.

Introduction

The experimental systems we discuss are based upon the experiments carried out by Lu *et al.*[1] In order to explain the results of experiments, Lu *et al.* offered a simulation model having various parameters ambiguous in physical meanings, and tried to explain various physical properties of polymerization systems. But there have been somewhat exposed the discrepancy between their theory and experimental data, which results from the fact that their theory did not considered the effects of interaction between polymer-polymer and polymer-oligomer. In our work, six interaction parameters of Lu *et al.* are transformed into five topological interaction functions clear in physical meanings, and there has been offered a more desirable and general topological theory which can obtain the values of physical properties of general dispersion polymerization systems over all the temperature areas.

The theories which have systematically studied the physical properties of polymers so far are the phantom n etwork theories[2,3] headed by Flory *et al.* and the topological network theories[4,6] headed by Iwata *et al.* Topological network theories have developed re markably since these have explained very well the effect of interaction between chains by entanglement. Thus topological theories have recently played a great role in studying various physical properties including the elasticity of polymers.

Iwata has theoretically explained the various phenomena of polymer networks by applying topological theories to a polymer system which consists of only a single kind of polymers.[4~6] The models which he has offered are mainly confined to the SCL (simple cubic lattice) models,[5,6] and he did not obtain nor offer detailed transformation matrices and related topological distribution functions about the THL (tetrahedral lattice) model. It has been known that for most polymer systems the structure of polymer networks takes the shape of the THL type rather than that of the SCL type.[4~6] Therefore, in view of extending the topological theory of Iwata to the THL model, we offered detailed transformation matrices about the THL model and related topological distribution functions in our previous work.[7~9]

Topological Theory for Dispersion Systems

It is well known that polymers in the solid or melt state have the structure of such a lattice as the THL (tetrahedral lattice) model.[7~9] But studies on polymerization systems (*i.e.*, emulsion, dispersion, suspension or solution polymerization) have been given few. It can be assumed that the structure of polymers in particles has such a lattice model as the THL model whether the reaction of polymerization progresses or not. The gist of the present work consists of applying a topological theory to the dispersion polymerization system by assuming that all the polymers in each particle form the polymer network by combination of neighboring polymer chains, and especially have the structure of a THL model. The polymerization system we deal with is based upon the results of experiments of Lu *et al.* about the dispersion polymerization of styrene in ethanol. Concretely speaking, it is assumed that polymer chains in each particle take the form of the THL model formed in tetrahedral combination mode around each junction point.

For the dispersion polymerization of monomers in a diluent, polymer chains in each particle can form a polymer network caused by the cross-link between polymer molecules. Also there can arise topological interaction caused by entanglement between an oligomer and a polymer. Among polymer chains topological interaction can arise by entanglement caused by single or double contact. Among oligomers and polymer chains topological interaction can arise from entanglement caused by single contact.

The THL model is the one in which the junction points of polymer networks are located at the points of a body-centered cubic lattice, and in which the arrangement of four st rands projected from each junction point always takes the tetrahedral structure.

The distribution functions and transformation matrices about the THL model had already been offered by our pre-

vious work.[7~9] The study about the physical properties of polymer blends and polymer solutions had also been carried out, based on the THL model in our previous works.[10,11]

In the present work, five topological interaction terms caused by interaction between polymers and oligomers have been derived from topological distribution functions by assuming that the structure of polymer chains in each particle forms a large aggregate of the THL model.

All the systems we consider in this work are dispersion polymerization systems in which styrene is a monomer, and ethanol is a diluent. In the THL model, it is supposed that a polymer chain aggregate is regularly arranged at the lattice points, in turn with the solvent-oligomer aggregate. The network structure of the THL model is composed of the aggregate of polymer chains and molecules of low molecular weight (*i.e.*, monomer, diluent or oligomer). See Refs. 7-11 for the detailed parts of the THL model.

For the THL model, the single contact probability between two strands, $g_p(r_i)$, and double one between two strands, $h_p(r_i)$, are given by[7~9]

$$g_p(r_i)=m^{-2}\sum_{\mu=1}^{m^2}P_{ph}(O_\mu|r_i)$$

$$h_p(r_i)=m^{-2}[g_p(r_i)]^{-1}\sum_{\mu=1}^{m^2}\sum_{\mu'=1}^{m^2}P_{ph}(O_{\mu\mu'}|r_i) \quad (1)$$

where m is the number of submolecules in a strand, and r_i is the position vector of the ith strand from the reference junction point. $P_{ph}(O_\mu|r_i)$ is the single contact distribution function between chains, and $P_{ph}(O_{\mu\mu'}|r_i)$ is the double one of the phantom network. The detailed terms of $P_{ph}(O_\mu|r_i)$ and $P_{ph}(O_{\mu\mu'}|r_i)$ have been offered in Refs. 7-9.

As shown previously in our work,[11] the number of distinguishable arrangement caused by single contact among all the polymer strands, Ω_g, is given by

$$\Omega_g=\Omega_{FH}\ \varepsilon_m\ \ln[(1-\phi)^{1/4}/(1-\phi-0.5\phi^2)^{3/4}]. \quad (2)$$

And the number of distinguishable arrangement caused by double contact among all the strands, Ω_h, is represented by

$$\Omega_h=\Omega_{FH}\ \varepsilon_m\ \ln[(1-\phi)^{1/4}/(1-\phi-0.5\phi^2)^{1/2}]. \quad (3)$$

In Eqs. (2) and (3), $\phi(r)$ is the l ocal polymer volume fraction at r from the reference point. The number of distinguishable arrangement of the Flory-Huggin's theory, Ω_{FH}, and the variable ε are given by

$$\Omega_{FH}=(1/n_1!)[\{z(z-1)^{m-2}\}n_0^{m-1}]^{n1} \quad (4)$$

and

$$\varepsilon=(1/4)\ (\nabla^2\phi)_0\alpha^2 n_0 \quad (5)$$

where z is the coordination number of the lattice, n_0 is the number of the lattice sites, n_1 is the number of lattice sites available to the $(i+1)$th strand, and a is the length of a strand. As offered previously, m is the number of submolecules contained in a strand. The number 4 in the denominator of Eq. (5) represents four directions of the strands attached to junction points. Thus the total number of topologically distinguishable arrangements caused by polymer-polymer entanglement, $\Omega_{pp,top}$, plays a great role in evaluating the values of physical properties. Since for polymer-polymer entanglement, the contributional terms of single and double contact are all important, for polymer-polymer entanglement $\Omega_{pp,top}$ can be written by

$$\Omega_{pp,top}=\Omega_g+\Omega_h$$
$$=\Omega_{FH}\ \varepsilon m\ \ln\ [(1-\phi)^{1/2}/(1-\phi-0.5\phi^2)^{5/4}]. \quad (6)$$

For oligomer-polymer entanglement since the length of oligomer chains is shorter than that of polymer chains, and the contributional term of only single contact has an important meaning, $\Omega_{op,top}$ can be represented by

$$\Omega_{op,top}=\Omega_g$$
$$=\Omega_{FH}\ \varepsilon m\ \ln\ [(1-\phi)^{1/4}/(1-\phi-0.5\phi^2)^{3/4}]. \quad (7)$$

Eqs. (6) and (7) are very valuable expressions obtained by expanding the topological theory of Iwata to the THL model. The topological interaction between polymer-polymer chains or polymer-olimer chains arises from entanglement between the related strands. The degree of polymerization and the molecular weight distribution are affected by the interaction which was caused by entanglement between strands in the polymer network. For the theory of Lu *et al.*, there was not considered the topological effect caused by interaction between strands.

Essentially the greater the length of a chain is, the greater the tendency to form polymer networks is, and usually it is apt to have the network structure composed of junction points of the four functional type. The theory of Lu *et al.* is not only a semiqu antitive theory on dispersion polymerization systems but also an incomplete theory having not considered the contributional effect between junction points and strands. In the present work, we modify an incomplete part of theirs, based upon topological network theories, and offer a general and inclusive theory applicable to all the dispersion polymerization systems.

For phantom network theories, the entropy of polymer systems has been analyzed so far only by contributional terms caused by displacement of junction points. In topological network theories, the change of entropy and free energy has been more completely considered by adding the distribution terms of entropy caused by interaction among strands to those caused by displacement of junction points.

Eqs. (6) and (7) have important meaning in the fact that those offer the source of topological interaction energy based upon the structure of the polymer network of the THL model. In the next section, we consider how Eqs. (6) and (7) contribute to expanding the theory of Lu *et al.*, and how it explains agreement between theoretical values and experimental data.

Consider a polymer network of the THL model, composed of n_A polymer molecules and n_B molecules of low molecular weight (*i.e.*, oligomer, diluent, and monomer) in a particle of the volume V.

Let the number of junction points of polymer chains be n_{AJ}, and that of small molecule chains be n_{BJ}, then the total number of junction points of the polymer network, n_J, is given by

$$n_J=n_{AJ}+n_{BJ}. \quad (8)$$

The partition function of junction points in a phantom network, Ω_{ph}, is given by[11]

$$\Omega_{ph}=\Omega_{FH}[1+(\varepsilon m/2)\ \ln\{1-\bar{\phi}\}^{-1}] \quad (9)$$

where $\bar{\phi}$ is the averaged polymer concentration, m is the number of the submolecules contained in a strand, and Ω_{FH} is given in Eq. (4). The total partition function of the mixed polymer-polymer systems, pp, is obtained by adding Eq. (9) to Eq. (6). Namely,

$$\Omega_{pp}=\Omega_{ph}+\Omega_{pp,top}$$
$$=\Omega_{FH}[1+(5\varepsilon m/4)\ln\{1-\bar{\phi}-\bar{\phi}^2\}^{-1}]. \quad (10)$$

The total partition function of the mixed polymer-oligomer systems, Ω_{op}, is obtained by adding Eq. (9) to Eq. (7) as follows;

$$\Omega_{op}=\Omega_{ph}+\Omega_{op,top}$$
$$=\Omega_{FH}[1+(\varepsilon m/2)\ \ln\{(1-\bar{\phi})^{1/2}\ (1-\bar{\phi}-0.5\bar{\phi}^2\}^{-3/2}\}]. \quad (11)$$

The dispersion polymerization system of styrene in ethanol is composed of a single polymer component (polystyrene) in a binary solvent mixture (styrene and ethanol). In principle, the thermodynamic treatment of the equilibrium distribution of each component between continuous phase and polymer particle phase is based on the Flory-Huggins's theory, and Morton[12] extended their theory to include the interfacial free energy. Since ethanol may diffuse into the polymer particles and alter the monomer partitioning, the partial molar free energy of ethanol is considered in this thermodynamic model.

At equilibrium, the partial molar free energy of styrene and ethanol absorbed in the polymer phase is equal to their partial molar free energy in continuous phase as follows;

$$(\Delta G_m/RT)_c=(\Delta G_m/RT)_p$$
$$(\Delta G_e/RT)_c=(\Delta G_e/RT)_p \quad (12)$$

where the subscripts m, e, c, and p represent styrene, ethanol, continuous phase, and polymer phase, respectively. Based on the assumption that the continuous phase contains a negligible amount of polymer, Lu *et al.* offered two thermodynamic equations for the styrene monomer system and the ethanol solvent system, respectively, as follows;

$$\ln(\phi_{mp})+(1-M_{me})\phi_{ep}+(1-M_{mp})\phi_{pp}+\chi_{me}\phi_{ep}^2+\chi_{mp}\phi_{pp}^2$$
$$+\phi_{ep}\phi_{pp}(\chi_{me}+\chi_{mp}-\chi_{ep}M_{me})+2\gamma\ \bar{V}_m/rRT-\ln(\phi_{mc})$$
$$-(1-M_{me})\phi_{ec}-\chi_{me}\phi_{ec}^2=0 \quad (13)$$

$$\ln(\phi_{ep})+(1-M_{em})\phi_{mp}+(1-M_{ep})\phi_{pp}+\chi_{em}\phi_{mp}^2+\chi_{ep}\phi_{pp}^2$$
$$+\phi_{mp}\phi_{pp}(\chi_{em}+\chi_{ep}-\chi_{mp}M_{em})+2\gamma\ \bar{V}_e/rRT-\ln(\phi_{ec})$$
$$-(1-M_{em})\phi_{mc}-\chi_{em}\phi_{mc}^2=0 \quad (14)$$

where

$$M_{me}=\bar{V}_m/\bar{V}_e,\ M_{mp}=\bar{V}_m/\bar{V}_p,\ M_{em}=1/M_{me},\ M_{ep}=\bar{V}_e/\bar{V}_p,$$
$$\chi_{me}=\bar{V}_m(\delta_e-\delta_m)2/RT,\ \text{and}\ \chi_{em}=\chi_{me}M_{em}. \quad (15)$$

In Eqs. (13)-(15), $\bar{V}_e$ is the molar volume of ethanol diluent, $\bar{V}_m$ is the molar volume of styrene mon omer, and $\bar{V}_p$ is the molar volume of polystyrene. The unit of $\bar{V}_e$, $\bar{V}_m$, and $\bar{V}_p$ is all cm^3mol^{-1}. ϕ_{ec} is the volume fraction of ethanol in continuous phase, ϕ_{mc} is the volume fraction of styrene in continuous phase, ϕ_{pc} is the volume fraction of polystyrene in continuous phase, ϕ_{ep} is the volume fraction of ethanol in polymer phase, ϕ_{mp} is the volume fraction of styrene in polymer phase, and ϕ_{pp} is the volume fraction of polystyrene in polymer phase. δ_m is the solubility parameter of styrene, δ_e is the solubility parameter of ethanol, and δ_p is the solubility parameter of polystyrene. The unit of δ_m, δ_e, and δ_p is all $(cal/cm^3)^{1/2}$. χ_{em} is the interaction parameter of ethanol and styrene, χ_{ep} is the interaction parameter of ethanol and polystyrene, χ_{me} is the interaction parameter of styrene and ethanol, and χ_{mp} is the interaction parameter of styrene and polystyrene. γ is the interfacial tension of the styrene in dyn/cm unit.

Lu *et al.* have solved the above thermodynamic equations by numerical methods to simulate the styrene partitioning behavior in the dispersion polymerization of styrene in ethanol, based on the material balences of styrene, ethanol, and polystyrene in each phase. The total number of particles in the polymerization system should be determined to obtain the size of monomer-swollen particles. This value can be obtained by the final particle diameter, which is usually measured by scanning electron microscopy. In usual, the total number of particles remains constant after the particle nucleation stage which was completed at an early stage of the reaction (about 1% conversion).

In this thermodynamic model, Lu *et al.* have introduced four interaction parameters χ_{em}, χ_{ep}, χ_{me}, and χ_{mp} ambiguous in physical meanings, and made theoretical simulations by using these parameters. They have not offered reasonable and detailed equations for these parameters, and have not suggested general formulation applicable to all kinds of dispersion polymerization systems. Thus their theoretical model seems to be semiquantitive and incomplete model.

In the present work, we extend the theory of Lu *et al.* so as to transform their theory into more complete form. Lu *et al.* regared χ_{em} and χ_{me} as two separate parameters, while we have let χ_{em} and χ_{me} be only a parameter, assuming that χ_{em} is equal to χ_{me} in physical meanings. Now it is time to offer reasonable and detailed equations for three parameters (χ_m, χ_{ep}, and χ_{mp}) to convert these parameters into three topological interaction functions, and to suggest general formulation applicable to all kinds of dispersion polymerization systems. Consider the dispersion polymerization system of styrene in ethanol. It is necessary to introduce the concept of the contact velocity between materials (*i.e.*, ethanol-styrene, ethanol-polystyrene, and styrene-polystyrene) in order t o convert three parameters (χ_m, χ_{ep}, and χ_{mp}) into three topologically quanti tive expressions. In a view of topological theories, the word *contact velocity* is defined as the average velocity at which n moving couples of materials of having the given molecular volume collide with each other under the given diffusion velocity and concentrations. The values of contact velocity are proportional to the multiplication of diffusion coefficients, concentrations, molecular number density, the distances of centers materials. The interaction function χ_m is proportional to $\bar{V}_m$ and V_{em}, but is inversely to temperature. χ_{ep} is proportional to the interfacial tension around each particle. And χ_{mp} is proportional to V_{mp} and the interfacial tension around each particle. Thus, based upon the topological model, the contact velocity between ethanol and styrene, V_{em}, can be defined as follows;

$$V_{em}=(4\pi/n)\left(\sum_{j=1}^{n} d_j\right)\cdot N_m N_e \sum_{j=1}^{m} D_{ej}D_{mj}P_{ej}P_{mj}. \quad (16)$$

And the contact velocity between ethanol and polystyrene, V_{ep}, can be obtained by

$$V_{ep}=(4\pi/n)\Big(\sum_{j=1}^{n} d_j\Big)\cdot N_p N_e \sum_{j=1}^{m} D_{ej}D_{pj}P_{ej}P_{pj}. \quad (17)$$

Simarly to Eqs. (16) and (17), the contact velocity between styrene and polystyrene, V_{mp}, can be given by

$$V_{mp}=(4\pi/n)\Big(\sum_{j=1}^{n} d_j\Big)\cdot N_m N_p \sum_{j=1}^{m} D_{mj}D_{pj}P_{mj}P_{pj}. \quad (18)$$

In Eqs. (16)-(18), n represents the number of interaction couples, and d_j is the distance between centers of jth couple materials. N_m, N_e, and N_p represent the number density of molecules of styrene, that of ethanol, and that of polystyrene, respectively. D_e, D_m, and D_p represent the diffusion coefficients of ethanol, styrene, and polystyrene, respectively. P_e, P_m, and P_p represent the concentrations of ethanol, styrene, and polystyrene, respectively.

The interaction function χ_m is proportional to $\overline{V}_m$ and V_{em}, but is inversely proportional to temperature. χ_{ep} is proportional to the interfacial tension around each particle. And χ_{mp} is V_{mp} and the interfacial tension around each particle.

Then rewriting the interaction functions in view of topological theories,[4~9] χ_m, χ_{ep}, and χ_{mp} can be given as follows;

$$\chi_m=(1/4)\cdot\overline{V}_m/RT\cdot V_{em}$$
$$=(1/4)\cdot\overline{V}_m/RT\cdot(4\pi/n)\Big(\sum_{j=1}^{n} d_j\Big)\cdot N_m N_e \sum_{j=1}^{m} D_{ej}D_{mj}P_{ej}P_{mj}$$

$$\chi_{ep}=(1/4)\cdot\gamma\ V_{ep}$$
$$=(1/4)\cdot\gamma(4\pi/n)\Big(\sum_{j=1}^{n} d_j\Big)\cdot N_p N_e \sum_{j=1}^{m} D_{ej}D_{pj}P_{ej}P_{pj}$$

$$\chi_{mp}=(1/4)\cdot\gamma\ V_{mp}$$
$$=(1/4)\cdot\gamma(4\pi/n)\Big(\sum_{j=1}^{n} d_j\Big)\cdot N_m N_p \sum_{j=1}^{m} D_{mj}D_{pj}P_{mj}P_{pj}. \quad (19)$$

In addition to the three interaction functions χ_m, χ_{ep}, and χ_{mp}, we introduced two new topological functions χ_{op} and χ_{pp}. χ_{op} is the interaction function between oligomers and polymers, and χ_{pp} is the interaction function between polymers themselves. These functions χ_{op} and χ_{pp} are proportional to the natural logarithms of partition functions of polymer systems. For the THL model, since the free energy of dispersion polymerization system is proportional to a natural logarithm of partition functions, topological interaction functions χ_{pp} and χ_{op} can be given as follows;

$$\chi_{pp}=(1/12)\ \ln\ \Omega_{pp,top}$$
$$=(1/12)\ \ln[\Omega_{\mathrm{FH}}\ \varepsilon_m\ \ln\ \{(1-\phi)^{1/2}/(1-\phi-0.5\phi^2)^{5/4}\}] \quad (20)$$

and

$$\chi_{op}=(1/12)\ \ln\ \Omega_{op,top}$$
$$=(1/12)\ \ln[\Omega_{\mathrm{FH}}\ \varepsilon_m\ \ln\ \{(1-\phi)^{1/4}/(1-\phi-0.5\phi^2)^{3/4}\}] \quad (21)$$

where the local polymer volume fraction, $\phi(r)$, as a function of radius (r) of gyration is assumed to be expressed as a Taylor series in terms of the volume fraction at 0 (the reference point).[11]

$$\phi(r)=\phi_0+[(r\cdot\nabla)\Phi]_0+(1/2)[(r\cdot\nabla)^2\Phi]_0. \quad (22)$$

For the THL model, the average volume fraction at a distance r from randomly chosen lattice site can be expressed as

$$\Phi(r)=\Phi_{AV}+(1/4)(\nabla^2\Phi)_0 r^2 \quad (23)$$

where Φ_{AV} is the volume fraction averaged over the n_o sites. Then Eq. (22) is transformed as follows;

$$\phi(r)=\phi_0+[(r\cdot\nabla)\{\Phi_{AV}+(1/4)(\nabla^2\Phi)_0 r^2\}]_0+(1/2)[(r\cdot\nabla)^2 \cdot\{\Phi_{AV}+(1/4)(\nabla^2\Phi)_0 r^2\}]_0. \quad (24)$$

Then finally Eqs. (20) and (21) are transformed as follows;

$$\chi_{pp}(r)=(1/12)\ \ln\ \Omega_{pp,top}$$
$$=(1/12)\ \ln[\Omega_{\mathrm{FH}}\ \varepsilon_m\ \ln\{(1-\phi_0-[(r\cdot\nabla)\{\Phi_{AV}+(1/4)(\nabla^2\Phi)_0 r^2\}]_0-(1/2)[(r\cdot\nabla)^2\cdot\{\Phi_{AV}+(1/4)\cdot(\nabla^2\Phi)_0 r^2\}]_0)^{1/2}/(1-\phi_0-[(r\cdot\nabla)\{\Phi_{AV}+(1/4)(\nabla^2\Phi)_0 r^2\}]_0-(1/2)[(r\cdot\nabla)^2\cdot\{\Phi_{AV}+(1/4)\cdot(\nabla^2\Phi)_0 r^2\}]_0)-0.5<\phi_0+[(r\cdot\nabla)\{\Phi_{AV}+(1/4)\cdot(\nabla^2\Phi)_0 r^2\}]_0+(1/2)[(r\cdot\nabla)^2\cdot\{\Phi_{AV}+(1/4)(\nabla^2\Phi)_0\cdot r^2\}]_0>^2)^{5/4}\}] \quad (25)$$

and

$$\chi_{op}(r)=(1/12)\ \ln\ \Omega_{op,top}$$
$$=(1/12)\ \ln[\Omega_{\mathrm{FH}}\ \varepsilon_m\ \ln\ \{(1-\phi_0-[(r\cdot\nabla)\{\Phi_{AV}+(1/4)(\nabla^2\Phi)_0 r^2\}]_0-(1/2)[(r\cdot\nabla)^2\cdot\{\Phi_{AV}+(1/4)\cdot(\nabla^2\Phi)_0 r^2\}]_0)^{1/4}/(1-\phi_0-[(r\cdot\nabla)\{\Phi_{AV}+(1/4)(\nabla^2\Phi)_0 r^2\}]_0-(1/2)[(r\cdot\nabla)^2\cdot\{\Phi_{AV}+(1/4)\cdot(\nabla^2\Phi)_0 r^2\}]_0)-0.5<\phi_0+[(r\cdot\nabla)\{\Phi_{AV}+(1/4)\cdot(\nabla^2\Phi)_0 r^2\}]_0+(1/2)[(r\cdot\nabla)^2\cdot\{\Phi_{AV}+(1/4)(\nabla^2\Phi)_0\cdot r^2\}]_0>^2)^{3/4}\}]. \quad (26)$$

In Eqs. (25) and (26), the coefficient 1/12 corresponds to the number of twelve hexagonal loops producible around any junction point.[7~9] Therefore, in the THL model, the two thermodynamic equations for the styrene and the ethanol solvent system can be given as follows;

$$\ln(\phi_{mp})+(1-M_{me})\phi_{ep}+(1-M_{mp})\phi_{pp}+\chi_{me}\phi_{ep}^2+(\chi_{mp}+\chi_{pp})\phi_{pp}^2 +\phi_{ep}\phi_{pp}(\chi_m+\chi_{mp}+\chi_{op}-\chi_{ep}M_{me})+2\gamma\overline{V}_m/rRT-\ln(\phi_{mc}) -(1-M_{me})\phi_{ec}-\chi_m\phi_{ec}^2=0 \quad (27)$$

and

$$\ln(\phi_{ep})+(1-M_{em})\phi_{mp}+(1-M_{ep})\phi_{pp}+\chi_m\phi_{mp}^2+(\chi_{mp}+\chi_{pp})\phi_{pp}^2 +\phi_{mp}\phi_{pp}(\chi_m+\chi_{mp}+\chi_{ep}-\chi_{mp}M_{em})+2\gamma\overline{V}_e/rRT-\ln(\phi_{ec}) -(1-M_{em})\phi_{mc}-\chi_m\phi_{mc}^2=0. \quad (28)$$

Now it is time to represent the volume fraction functions (ϕ_{pc}, ϕ_{mc}, and ϕ_{ec}) into the form of topological functions of the THL model. Let r_c be the ratio of conversion, then the volume fractions can be transformed into functions of r_c as follows;

$$\phi_{pc}(r_c)=\phi_0+[(r_c\cdot\nabla)\{\Phi_{AV}+(1/4)(\nabla^2\cdot<(T/T_0-1)^{-1}\cdot\xi\ \overline{V}_p\cdot r_c^2>)\}] +(1/2)[(r_c\cdot\nabla)^2\{\Phi_{AV}+(1/4)(\nabla^2\cdot<(T/T_0-1)^{-1}\cdot\xi\ \overline{V}_m\cdot r_c^2>)\}] \quad (29)$$

$$\phi_{mc}(r_c)=\phi_0+[(r_c\cdot\nabla)\{\Phi_{AV}+(1/4)(\nabla^2\cdot<(T/T_0-1)^{-1}\cdot\xi\ \overline{V}_m\cdot r_c^2>)\}]+(1/2)[(r_c\cdot\nabla)^2\{\Phi_{AV}+(1/4)(\nabla^2\cdot<(T/T_0-1)^{-1}\cdot\xi\ \overline{V}_m\cdot r_c^2>)\}] \quad (30)$$

$$\phi_{pc}(r_c)=\phi_0+[(r_c\cdot\nabla)\{\Phi_{AV}+(1/4)(\nabla^2\cdot<(T/T_0-1)^{-1}\cdot\xi\ \overline{V}_e\cdot r_c^2>)\}]+(1/2)[(r_c\cdot\nabla)^2\{\Phi_{AV}+(1/4)(\nabla^2\cdot<(T/T_0-1)^{-1}\cdot\xi\ \overline{V}_e\cdot r_c^2>)\}]. \quad (31)$$

In Eqs. (29)-(31), ξ is a controlling parameter, T is the temperature of the system, T_0 is the reference temperature of the system.

Now if we represent the molecular distribution function, $M_w(r_c)$, from our previous work,[10] then

$$M_w(r_c)=(1/V)\{<M_m(r_c)\ M_p(r_c)>/<\rho_m(r_c)/\rho_p(r_c)>\}^{1/2}\cdot[\{1+\alpha\Psi(r_c)P(r_c)<\rho_m(r_c)\cdot M_m(r_c)/\rho_p(r_c)\cdot M_p(r_c)>^{1/2}\}\cdot\{1+\alpha\Psi(r_c)P(r_c)<\rho_p(r_c)\cdot M_p(r_c)/\rho_m(r_c)\cdot M_m(r_c)>^{1/2}\}]^{\mp1} \quad (32)$$

where α is a normalized constant, M_m is the molecular weight of low chain molecules, M_p is that of polymer molecules in each particle, ρ_m is the density of low chain molecules, ρ_p is the one of polymer molecules, Ψ is the solute-solvent distribution parameter, P is the chain contact distribution function, and V is the volume of the polymer-solvent system. (See Ref. 10 for more detailed parts.)

Eqs. (19)-(32) are the gist of our present work and the most important parts obtained by applying the THL model of topological theories to thermodynamical systems. Shortly speaking, the theory of Lu *et al.* is represented as Eqs. (13) and (14), while our theory has been given in Eqs. (22)-(32).

In the next section, we will explain the experimental results of Lu *et al.* based on our topological theory, and discuss the difference between the theory of Lu *et al.* and our own's.

Results and Discussion

The theory of Lu *et al.* for dispersion polymerization systems has been expa nded by introducing a topological network theory of dealing with the interaction between strands. It is assumed that the dispersion polymerization systems considered here are composed of the polymer networks of the THL model.

It can be regarded that the THL model offered here is the reasonable structure of polymer networks when attractive and repulsive forces between chains are all considered. For polymer networks of the THL structure, the gist of topological network theories is based on the fact that the interaction between strands is regarded as the principal contribution term to entropy and free energy for each polymer particle. Interaction between strands can be classified into the terms caused by single contact and those by double. A distance between the centers of strands, d, is defined as

$$d=|r_a+r_a'-r_b-r_b'|/2a\sqrt{m} \quad (33)$$

where r_a and r_a' are the position vectors representing both end points of the a strand, and r_b and r_b' those of the b strand. $g_p(r)$ and $h_p(r)$ of Eq. (1) can be readily transformed into $g_p(d)$ and $h_p(d)$, respectively. In Table 1, there are offered the experimental samples of Lu *et al.* for the dispersion polymerization of styrene in etanol.[1]

Table 1. The recipes of Lu *et al.* for the dispersion polymerization of styrene in ethanol (cited from Ref. 1)

sample component	SA	SB	SC	SD	SE	SF	SG
styrene (g)	50.0	50.0	50.0	50.0	50.0	50.0	25.0
ethanol (g)	150.0	150.0	150.0	150.0	150.0	150.0	150.0
ACPA (g)	1.0	0.5	0.25	0.5	0.5	–	–
AIBN (g)	–	–	–	–	–	0.5	0.25
PVPK-30 (g)	3.5	3.5	3.5	2.5	5.0	3.5	3.5
AOT 100 (g)	1.0	1.0	1.0	1.0	1.0	1.0	1.0

Note: ACPA=4,4′-azobis(4-cyanopentanoic acid); AIBN=2,2′-azobis(isobutyr-onitrile); PVP K-30=polyvinyl pyrrolidone K-30; AOT 100=aerosol di-2 ethyl hexyl ester of sodium sulfosuccinic acid.

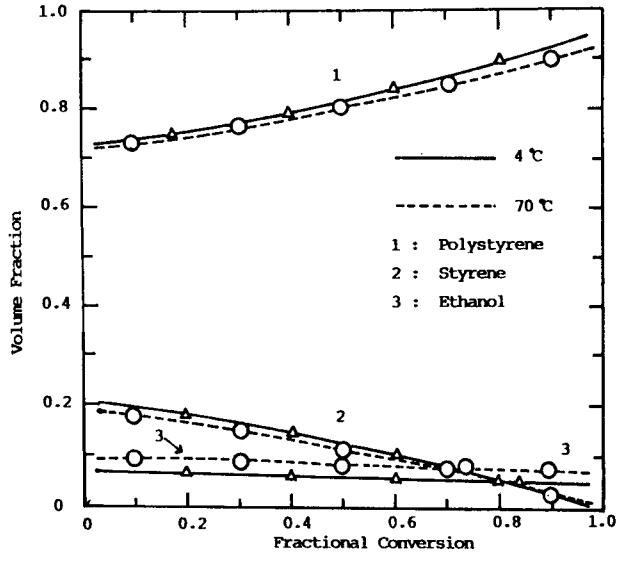

Figure 1. The curves calculated on the volume fraction of polystyrene (curve 1), styrene (curve 2) and ethanol (curve 3) in the polymer phase at 4 ℃(solid curve) and 70 ℃ (dotted curve). The symbols △ and ○ represent the experimental data points converted from Ref. 1.

As shown in Table 1, in two kinds of initiators (*i.e.*, ACPA [4,4′-azobis(4-cyanopentanoic acid)] and AIBN [2,2′-azobis (isobutyronitrile)]), the concentration effect of ACPA is greater than that of AIBN when the concentrations of two initiators and other materials are identical. When the concentration of the initiator is identical, the thinner the concentration of stabilizer is, the greater the mean size of particles is. In general, the larg er the size of polymer particles is, the smaller the values of number density of particles are. Since the larger the size of polymer chains is, the larger the effect of topological interaction between strands becomes, a sample (*i.e.*, sample SG) having higher values of $h_p(d)$ shows greater topological interaction between strands in polymer chains.

In this section, we will discuss our theoretical results by being divided into three parts.

Change of Component Materials versus Conversion Ratio at Constant Temperatures. In order to find

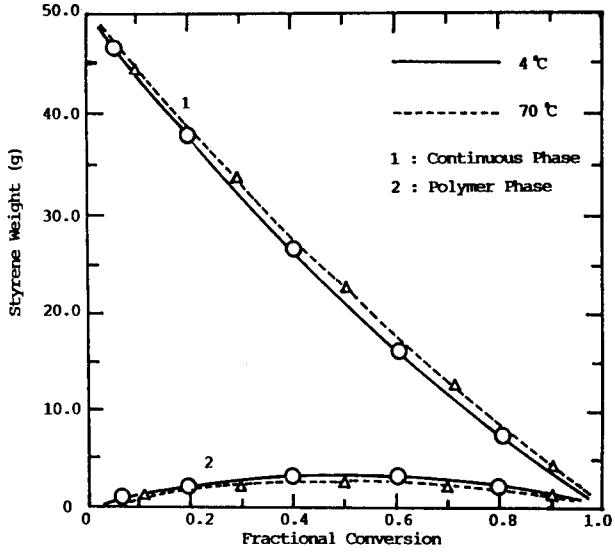

Figure 2. The curves calculated on styrene partitioning in continuous phase (curve 1) and polymer phase (curve 2) versus conversion at 4 ℃(solid curve) and 70 ℃ (dotted curve). The symbols △ and ○ represent experimental data points converted from Ref. 1.

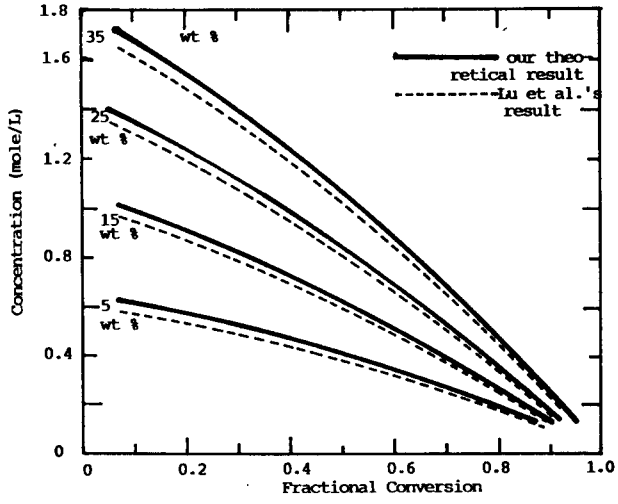

Figure 3. The curves calculated to consider the effect of initial styrene on concentration in polymer phase versus conversion at 70 ℃. The percentage of initial styrene concentration on styrene concentration in polymer phase is 35.0, 25.0, 15.0, 5.0 weight %, respectively, based on total weight. The solid curves represent the results of our theory, while the dashed curves represent those of the original theory of Lu *et al.* for dispersion polymerization systems. The variation of initial styrene concentration on styrene concentration in polymer phase becomes greater in our topological theory than in the original theory of Lu *et al.* It is regarded that such a tendency arises from the fact that in our theory there has been sufficiently considered the effect of interaction by entanglement between strands in polymer chains.

out how the topological interaction between strands affects the change of volume, weight or concentration of component materials versus conversion ratio, we have obtained the curves of Figures 1-3. Interaction between strands in each particle affects the change of volume of component materials (*i.e.*, polystyrene, ethanol, and styrene) in polymer phases (in Figure 1), the change of weight of styrene in continuous phases and polymer phases (in Figure 2), and the effect of initial styrene concentration (in Figure 3).

In Figure 1, there are shown the curves which were calculated on the volume fraction of polystyrene (curve 1), styrene (curve 2), and ethanol (curve 3) in the polymer phase at 4 ℃(solid curve) and 70 ℃ (dotted curve). The symbols in graphs represent the experimental data points converted from Ref. 1. The calculated volume fraction has been obtained from Eqs. (29)-(31). The values of parameters used in obtaining the curves of Figure 1 are given as follows;

$$\xi=0.274,\ \Phi_{AV}=1.289\times10^{-3} \text{ at } 4\ ℃$$
$$\xi=0.261,\ \Phi_{AV}=1.315\times10^{-3} \text{ at } 70\ ℃.$$

It is regarded that the controlling parameter ξ reflects the stabilization effect of the lattice formation of system materials at the given temperature. It seems that the value of Φ_{AV} reflects the fluidity of polymer chains having a given radius of gyration. Thus, we see that the lattice structure is stabler at 4 ℃ than at 70 ℃, and the fluidity of polymer chains is greater at 70 ℃ than at 4 ℃. If interaction between strands in each particle becomes great, then the value of ξ gets great, and that of Φ_{AV} gets small. As shown in Figure 1, as the conversion of styrene to polymers proceeds, the volume fraction of polystyrenes becomes greater, while those of styrene and ethanol get smaller. The calculated curves show a good agreement with the experimental data of Lu *et al.*

In Figure 2, there are shown the curves which were calculated on styrene partitioning in continuous phase (curve 1) and polymer phase (curve 2) versus conversion at 4 ℃ (solid curve) and 70 ℃ (dotted curve). The symbols △ and ○ represent the experimental data points converted from Ref. 1. The calculation of volume fraction has been obtained by continuous simulation method from Eqs. (27)-(28). The values of parameters used in solving Eqs. (27)-(28) are given as follows;

$$M_{me}=1.341,\ M_{mp}=0.382, \text{ and } M_{ep}=0.279.$$

For the THL model, interaction between strands in each particle can be classified into attractive and repulsive force. For dispersion polymerization systems, the greater the interaction of polymer strands is, the smaller the value of $\overline{V}_p$ is. Thus, the values of M_{mp} and M_{ep} decrease with increasing interaction between strands. In the while, the value of M_{me} is expected to change slightly.

From the calculation, we see that approximately 10 volume % (based on polymer phase) of ethanol is absorbed in the polymer particles. Also it is exposed that the absorbed ethanol is only a volume of around 0.1-1.0% of the total ethanol used. The amount of styrene in both polymer and continuous phases has been calculated by assuming that a negligible amount of ethanol is lost from the continuous phase to the polymer particles. The majority of styrene seems to remain in the continuous phase throughout the polymerization. As shown in Figure 2, as the conversion of styrene to polymers proceeds, the weight fraction of styrene becomes conspicuously smaller in continuous phase, while in polymer phase the

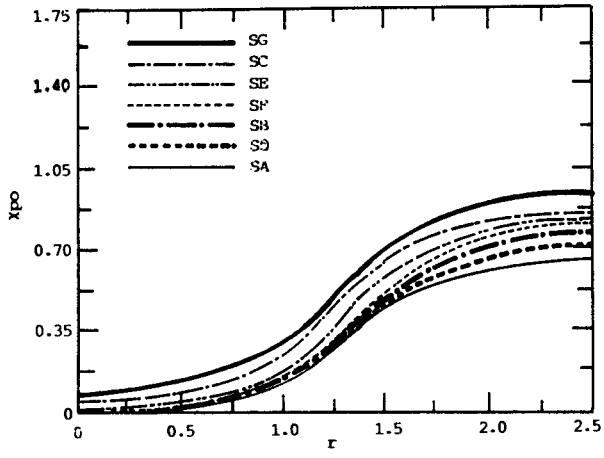

Figure 4. The calculated curves of interaction function on polymer-oligomer interaction, χ_{po}, as functions of mean radius of gyration, r at 70 ℃. The longer the length of chains is, the greater the probability of contact between neighbor chains is. Then the calculated values of χ_{po} become greater with increasing values of mean radius of gyration.

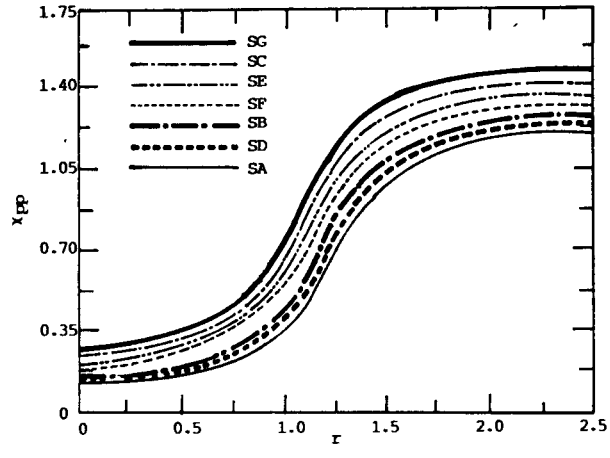

Figure 5. The calculated curves of interaction function on polymer-polymer interaction as functions of mean radius of gyration, r at 70 ℃. The longer the length of chains is, the greater the probability of contact between neighbor chains is. Then the calculated values of χ_{pp} become greater with increasing values of mean radius of gyration.

weight fraction of styrene changes monotonously. It is exposed that the calculated curves show a good agreement with the experimental data of Lu *et al.*

In Figure 3, there are shown the curves which were calculated to consider the effect of initial styrene concentration on styrene concentration in polymer phase versus conversion at 70 ℃. Similarly to Figure 2, the calculation of the change of initial styrene concentration has been obtained by continuous simulation method from Eqs. (27)-(28). The percentage of initial styrene concentration on styrene concentration in polymer phase is 35.0, 25.0, 15.0, and 5.0 weight %, respectively, based on total weight. It is shown that the styrene concentration in the polymer particles increases with increasing initial styrene concentration. As shown in Figure 3, it is apparent that the styrene concentration in the polystyrene particles is very low (1.5 mol/dm^3 at 5% conversion) and decreases further as the polymerization proceeds. The solid curves represent the results of our theory, while the dashed curves represent those of the original theory of Lu *et al.* for dispersion polymerization systems. The variation of initial styrene polymerization on styrene concentration in polymer phase becomes greater in our topological theory than in the original theory of Lu *et al.* It is regarded that such a tedency arises from the fact that in our theory there has been sufficiently considered the effect of interaction by entanglement between strands in polymer chains.

Calculation of Topological Interaction Functions versus Radius of Gyration. For dispersion polymerization systems, interaction between strands in each particle is composed of polymer-oligomer interaction and polymer-polymer interaction. In the present work, two new interaction parameters, $\chi_{pp}(r)$ and $\chi_{po}(r)$, have been derived for the first time. The graph for $\chi_{po}(r)$ is given in Figure 4, and that for $\chi_{pp}(r)$ is given in Figure 5. Interaction between strands affects the size of polymer molecules. It is expected that the greater the interaction of polymer strands is, the smaller the molecular weight of polymers is because interaction between strands may prevent each polymer molecule from growing further. Since the longer the length of chains with which contact each other is, the greater the contact probability is, then for a given radius of gyration the value of $\chi_{pp}(r)$ is always greater than that of $\chi_{po}(r)$.

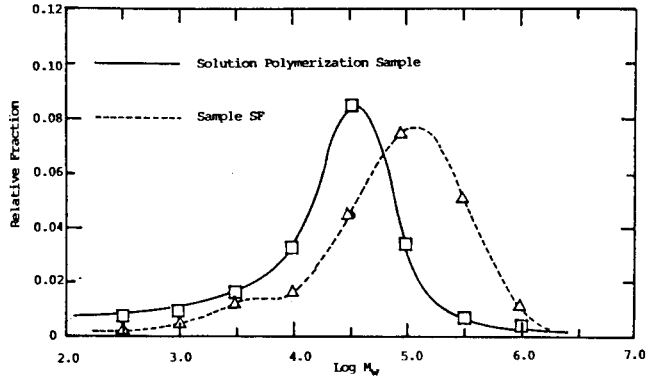

Figure 6. For solution polymerization and dispersion polymerization, the curves calculated on molecular weight distribution to consider the effect of polymerization modes. The symbols □ and △ represent the experimental data points of molecular weight distribution for the solution polymerization polymer obtained at 50% conversion and the final polymer obtained from dispersion polymerization (sample SF), respectively.

In Figure 4, there are shown the calculated curves of interaction function on polymer-oligomer interaction, χ_{po} [Eq. (26)], as functions of mean radius of gyration, r at 70 ℃. The longer the length of chains is, the greater the probability of contact between neighboring chains is. Then the calculated values of χ_{po} become greater with increasing values of mean radius of gyration.

In Figure 5, there are shown the calculated curves of interaction, χ_{pp} [Eq. (25)], on polymer-polymer interaction as functions of mean radius of gyration, r at 70 ℃. The longer

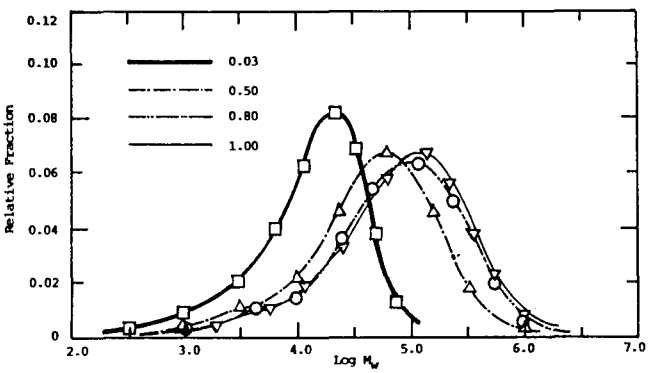

Figure 7. For various conversion, the curves calculated on molecular weight distribution of polymers prepared by re action SF. The symbols □, △, ○, and ₩ represent the experimental data points of molecular weight distribution of polymers obtained from conversion 0.03, 0.50, 0.80, and 1.00, respectively.[1]

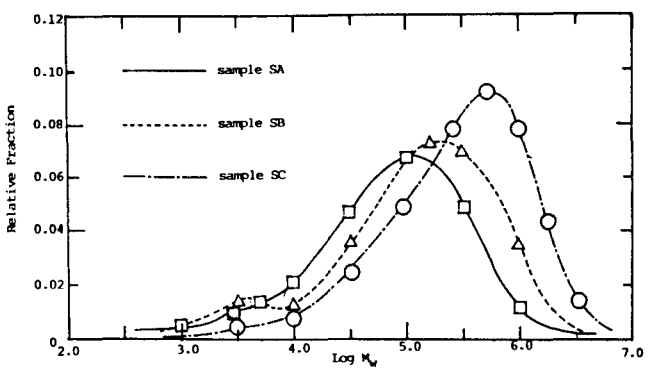

Figure 8. The curves calculated for the effect of ACPA initiator concentration on molecular weight distribution. The symbols □, △, and ○ represent the experimental data points of molecular weight distribution of the final polymers obtained from samples SA (2.0%), SB (1.0%), and SC (0.5%), respectively.[1]

the length of chains is, the greater the probability of contact between neighboring chains is, the greater the probability of contact between neighboring chains is. Then the calculated values of χ_{pp} become greater with increasing values of mean radius of gyration.

Effect of Topological Interaction versus Molecular Weight Distribution. The effect of topological interaction on molecular weight distribution is related to polymerization mode (in Figure 6), conversion ratio (in Figure 7), and the chemical composition of samples (in Figure 8). In Figure 9, there are shown the comparison of our theoretical result with Lu *et al.*'s.

In Figure 6, there are shown the curves which are calculated on molecular weght distribution to consider the effect of polymerization modes for solution polymerization and dispersion polymerization. The symbols □ and △ represent the experimental data points of molecular weight distribution for the solution polymerization polymer obtained at 50% conversion and the final polymer obtained from dispersion polymerization (smple SF), respectively. It is known that the molecular weight of the dispersion polymer at 3% conversion is more like that of the solution polymerization polymer at 50%

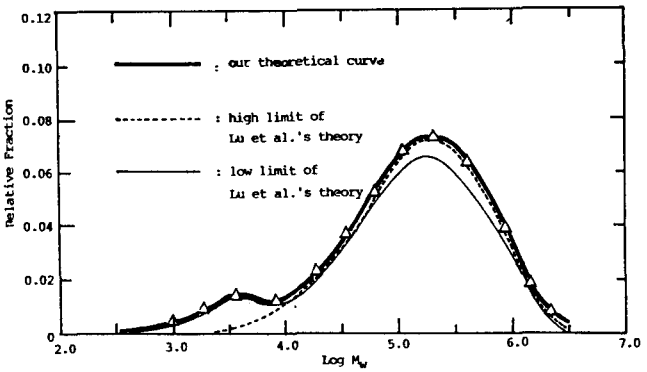

Figure 9. Comparison of our theoretical results with the experimental data for sample SB. The symbol △ represents the experimental data points. The thick solid line represents the curve calculated from our theory, while the dotted line represents the high limit curve of Lu *et al.*'s theory, and the thin solid line represents the low one of Lu *et al.*'s.

conversion and increases with increasing conversion. Such results suggest that a significant topological interaction can occur during the dispersion polymerization. The calculation of volume fraction has been obtained by continuous simulation method from Eqs. (29)-(32). As shown in Figure 6, the mean value of molecular weight of polymers of sample SF is greater than the one of solution polymerization polymers. It is shown that the calculated curves show a good agreement with the experimental data.[1]

In Figure 7, for various conversion, there are shown the curves which were calculated on molecular weight distribution of polymers prepared by reaction SF. The symbols □, △, ○, and ₩ represent the experimental data points of molecular weight distribution of polymers obtained from conversion 0.03, 0.50, 0.80, and 1.00, respectively. The values of parameters used in solving Eq. (32) are given as follows;

$$\alpha=0.738,\ \rho_m=0.681,\ \rho_p=0.928,\ \text{and}\ \Psi=0.674.$$

The values of weight average molecular weight versus conversion 0.03, 0.50, 0.80, and 1.00 are 2.2×10^4, 8.1×10^4, 1.2×10^5, and 1.3×10^5, respectively. As shown in Figure 7, the ratio the degree of conversion is, the broader the distribution of molecular weight is. It is exposed that the curves calculated from Eq. (32) are well fitted with the experimental data points of Lu *et al.*

If we consider the monomer partitioning study, we see that the majority of the styrene resides in the continuous phase. Since most of the initiator remains in equilibrium with the monomer and diluent in the continuous and polymer phases, most of the initiator is expected to stay in the continuous phase. Thus, it can be expected that the polymerization should proceed mainly in the continuous phase as a solution polymerization process.

In the result, the process of the polymerization and the molecular weight of final polymer found for dispersion polymerization should be close to those of solution polymerization at low conversion under the same reaction conditions. As a result, since some degree of topological interaction is apparent in the dispersion polymerization process, and the rate of polymerization deviates from that of solution polyme rization, it is indicated that polymerization within the mono-

Table 2. The values of physical parameters which are used to simulate monomer partitioning for all the samples

Temperature (℃)	$\overline{V}_m$ (cm³/mol)	$\overline{V}_e$ (cm³/mol)	χ_m	χ_{mp}	χ_{ep}
4	113.0	57.3	2.90	0.36	2.36
70	120.7	61.8	1.65	0.24	2.07

mer-swollen particles is also important.

In Figure 8, there are shown the curves which were calculated for the effect of ACPA initiator concentration on molecular weight distribution. The symbols □, △, and ○ represent the experimental data points of molecular weight distribution of the final polymers obtained from samples SA (2.0%), SB (1.0%), and SC (0.5%), respectively.[1] Since the activity of growing polymers becomes greater during dispersion polymerization as the concentration of ACPA initiator increases, then interaction between growing polymer-oligomer or growing polymer-polymer grows great. Thus the time interval of the termination step of polymerization becomes short, and the average molecular weight gets small with increasing initiator concentration. The values of parameters used in three samples are given as follows;

$\alpha=0.734$, $\rho_m=0.693$, $\rho_p=0.927$, and $\Psi=0.668$ for sample SA
$\alpha=0.736$, $\rho_m=0.687$, $\rho_p=0.931$, and $\Psi=0.672$ for sample SB
$\alpha=0.739$, $\rho_m=0.685$, $\rho_p=0.934$, and $\Psi=0.676$ for sample SC.

The calculation of relative fraction on molecular weight has been obtained from Eq. (32). As shown in Figure 9, the smaller the concentration of ACPA initiator is, the greater the mean values of molecular weight distribution are. We see that the calculated curves show a good agreement with the experimental data.

In Figure 9, there is shown the comparison of our theoretical results with the experimental data for sample SB. The symbol △ represents the experimental data points. The thick solid line represents the curve calculated from our theory, while the dotted line represents the high limit curve of Lu *et al.*'s theory, and the thin solid line represents the low one of Lu *et al.*'s.

For the original theory of Lu *et al.*, when their theoretical curve is fitted with experimental data in the upper ar ea of molecular weight distribution, the tracks of their theoretical curves deviate from the experimental data points of the lower area of molecular weight distribution. In the while, when their theoretical curve is fitted with experimental data in the lower area of molecular weight distribution, the tracks of their theoretical curves deviate from the experimental data points of the upper area of molecular weight distribution.

For our topological theory, it is regarded that the theoretically predicted results are well fitted with the experimental data. The discrepancy between Lu *et al.*'s theory and experimental data arises from the fact that their theory did not consider the topological interaction between polymer-polymer and polymer-oligomer in each particle.

As shown earlier, it is assumed that all the polymers in each particle form the lattice structure of the THL, and the topological interaction between polymers is composed of interaction between strands in the polymer network and of interaction between strands and oligomers.

In Table 2, there are shown the values of physical parameters and constants which are used to simulate monomer partitioning for all the samples. The physical meanings of these constants and parameters are self-evident.

Conclusion

The original theory of Lu *et al.* about polymerization systems has been expanded by considering topologically the contributional terms caused by the displacement of physically entangled points and junction points. Thus, for dispersion systems, our extended theory explains very well the characteristics of molecular weight distribution and the change of volume and concentration as functions of conversion. The dispersion polymerization systems considered here are supposed to have the structure of the THL network composed of polymer solutes and solvents. It is judged that the discrepancy between the experimental data and the original Lu *et al.*'s theory results from the fact that their original theory did not include the results of interaction caused by entangled points and junction points.

It is exposed that the results of the expanded theory show good agreement with the given experimental data. Finally, it is judged that the assumption of the THL structure for the given polymer systems is very reasonable, based upon the fact that the extended theory explains very well the given experimental data.

Acknowledgment. The Present Studies were Supported (in part) by the Basic Science Research Institute Program, Ministry of Education, 1995, Project No. BSRI-95-3414.

References

1. Lu, Y. Y.; El-Aasser, M. S.; Vanderhoff, J. W. *J. Polymer Sci.* **1988**, *26*, 1187.
2. Flory, P. J. *Proc. R. Soc. London Ser. A.* **1976**, *351*, 351.
3. Ziabicki, A.; Walasek, J. *Macromolecules* **1978**, *11*, 471.
4. Iwata, K.; Kurata, M. *J. Chem. Phys.* **1969**, *50*, 4008.
5. Iwata, K. *J. Chem. Phys.* **1980**, *73*, 562. **1981**, *74*, 2039. **1983**, *78*, 2778. **1985**, *83*, 1969.
6. Iwata, K. *J. Chem. Phys.* **1982**, *76*, 6363. **1982**, *ibid*, 6375.
7. Son, J. M.; Pak, H. *Proc. Coll. Natur. Sci., Seoul National University* **1988**, *13*, 47.
8. Son, J. M. *Ph. D. Thesis, Seoul National University, Seoul, Korea*, 1989.
9. Son, J. M.; Pak, H. *Bull. Korean Chem. Soc.* **1989**, *10*, 84.
10. Son, J. M.; Pak, H. *Bull. Korean Chem. Soc.* **1995**, *16*, 169.
11. Son, J. M.; Pak, H. *Bull. Korean Chem. Soc.* **1995**, *16*, 269.
12. Morton, M.; Kaizerman, S; Altier, M. W. *J. Colloid Sci.* **1954**, *9*, 300.